Heliyon 9 (2023) e14256

Contents lists available at ScienceDirect

Heliyon

journal homepage: www.cell.com/heliyon

Research article

A standardized pomegranate fruit extract ameliorates thioacetamide-induced liver fibrosis in rats via AGE-RAGE-ROS signaling

Hadeer M. Abouelezz [a,*], George S.G. Shehatou [a,b], Abdelhadi M. Shebl [c], Hatem A. Salem [a]

[a] Department of Pharmacology and Toxicology, Faculty of Pharmacy, Mansoura University, Mansoura, Egypt
[b] Department of Pharmacology and Biochemistry, Faculty of Pharmacy, Delta University for Science and Technology, Gamasa City, Egypt
[c] Department of Pathology, Faculty of Medicine, Mansoura University, Mansoura, Egypt

ARTICLE INFO

Keywords:
Thioacetamide
Liver fibrosis
Pomegranate fruit extract
Oxidative stress
RAGE
TGF-β1

ABSTRACT

This work aimed to investigate a possible mechanism that may mediate the hepatoprotective effects of pomegranate fruit extract (PFE) against thioacetamide (THIO)-induced liver fibrosis in rats. Male Sprague Dawley rats were randomly allocated into four groups (n = 8 each): control; PFE (150 mg/kg/day, orally); THIO (200 mg/kg, i.p, 3 times a week); and THIO and PFE-treated groups. Oral PFE treatment decreased liver/body weight ratio by 12.4%, diminished serum function levels of ALT, AST, ALP, LDH, and total bilirubin, increased serum albumin, boosted hepatic GSH (by 35.6%) and SOD (by 17.5%), and significantly reduced hepatic levels of ROS, MDA, 4-HNE, AGEs, and RAGE in THIO-fibrotic rats relative to untreated THIO group. Moreover, PFE administration downregulated the hepatic levels of profibrotic TGF-β1 (by 23.0%, $P < 0.001$) and TIMP-1 (by 41.5%, $P < 0.001$), attenuated α-SMA protein expression, decreased serum HA levels (by 41.3%), and reduced the hepatic levels of the fibrosis markers hydroxyproline (by 26.0%, $P < 0.001$), collagen type IV (by 44.3%, $P < 0.001$) and laminin (by 43.4%, $P < 0.001$) compared to the untreated THIO group. The histopathological examination has corroborated these findings, where PFE decreased hepatic nodule incidence, attenuated portal necroinflammation and reduced extent of fibrosis. These findings may suggest that oral PFE administration could slow the progression of hepatic fibrogenesis via reducing hepatic levels of AGEs, RAGE, ROS, TGF-β1, and TIMP-1.

1. Introduction

Liver fibrosis is an abnormal progressive deposition of extracellular matrix (ECM) proteins in hepatic parenchyma due to an imbalance that favors fibrogenesis over fibrinolysis [1,2]. Liver fibrosis and its more severe form, cirrhosis, are usually the inevitable result of chronic sustained liver damage caused by multiple injurious insults, including, but not limited to, infective viruses, autoimmune diseases, alcoholism, and metal ions overload [3]. Liver fibrosis is currently incurable, and its prevalence is increasing worldwide, thereby constituting a major health challenge to many countries globally [4,5].

* Corresponding author.
E-mail address: hadeer.abouelezz@mans.edu.eg (H.M. Abouelezz).

https://doi.org/10.1016/j.heliyon.2023.e14256
Received 29 July 2022; Received in revised form 22 February 2023; Accepted 28 February 2023
Available online 4 March 2023

The central event in hepatic fibrogenesis is the *trans*-differentiation of resident liver cells, predominantly quiescent hepatic stellate cells (HSCs), intomyofibroblasts (MFs), which promote the formation of excess scar tissue by both secreting ECM proteins and releasing inhibitors that mitigate ECM degradation, such as tissue inhibitor of metalloproteinase-1 (TIMP-1) [6]. TIMP-1 also exerts an anti-apoptotic influence on HSCs by enhancing their survival through increasing expression of B cell lymphoma 2 (Bcl-2) proteins [7,8]. The transforming growth factor-β1 (TGF-β1) cytokine, another important player in fibrogenesis, mediates HSC activation after a chronic injury, stimulates MF growth, and enhances ECM protein accumulation by reducing the production of interstitial collagenases and increasing expression of TIMP-1 and collagen-I [9,10].

Receptor for advanced glycation end products (AGEs) (RAGE) is a multiligand transmembrane receptor, which is expressed in HSCs and its expression is increased during HSC transition to MF phenotype [11–16]. Interaction of RAGE with various ligands, including AGEs, triggers oxidative stress, a major contributor to HSC activation, by activating downstream signaling cascades that include nuclear factor-κB (NF-κB), TGF-β1, NAD(P)H oxidase (NOX), and reactive oxygen species (ROS) [13,14,17–19]. Inhibition of the RAGE-mediated signal transduction has been suggested as a therapeutic target for chronic liver injury [16,20,21].

Pomegranate (*Punica granatum* L.) fruit has garnered great attention for many centuries owing to its health benefits [22], which has largely been attributed to its high content of polyphenols that include hydrolyzable tannins (particularly punicalagin) and anthocyanins [23,24]. Pomegranate-derived products are being investigated for potential use in the treatment of cardiovascular disease [25–27], Alzheimer's disease [28], benign prostatic hyperplasia [29], and cancer [30–32].

Pomegranate fruit extract (PFE), peel extract (PPE), juice (PJ), and seeds have demonstrated potent antioxidant properties [33]. It was reported that punicalagin, the major pomegranate component, displayed antioxidant activity against methotrexate-induced liver damage in mice [34]. Interestingly, PFE reduced serum AGE levels in high fat/high sucrose (HFHS)-fed mice and inhibited *in vitro* formation of AGEs from bovine serum albumin and sugars [35]. Furthermore, PFE reduced the vascular expression of TGF-β1 in obese Zucker rats [36].

Based on these reported activities of pomegranate products, we hypothesized that oral supplementation of PFE could attenuate the progression of liver fibrosis, induced by chronic thioacetamide (THIO) administration in rats, via interfering with the AGE-RAGE-ROS-TGF-β1-TIMP-1 cascade.

2. Materials and methods

2.1. Chemicals

TAA (catalog number 172502), Ellman's reagent [5, 5′-dithio-bis (2-nitrobenzoic acid)] (catalog number D218200), 2′, 7′-dichlorofluorescein diacetates (catalog number D6883, DCFDA), and all other chemical reagents were purchased from Sigma Aldrich (St. Louis, MO, USA).

Table 1
Compositional characteristics of pomegranate fruit extract (PFE) capsules (Pomella®) [39,40].

Physical characteristics	Specification
Plant part used	Fruit
Appearance	Dry powder
Color	Yellowish brown to brown
Odor and taste	Characteristic
Chemical analysis	
Assay for active constituents	
70% polyphenols including:	
a. Punicalagins	30%
b. Ellagic acid	5%
c. Gallic acid	0.3%
Solubility	
In water at 90 °C	
In alcohol	
Impurities	
Total heavy metals	<10 ppm
Lead	<0.5 ppm
Mercury	<2 ppm
Arsenic	<1 ppm
Microbiology	
Total plate count	<1000 cfu/g
Yeast and mold	<100 cfu/g
Escherichia coli	Absent
Salmonella typhi	Absent
Coliform	<10 cfu/g
Staphylococcus aureus	Absent
Enterobacteriaceae	Absent

ppm, part per million; cfu, colony forming unit.

2.2. Pomegranate fruit extract (PFE)

Standardized PFE capsules (Pomella®, 500 mg/capsule) were purchased from Verdure Science Inc. (Noblesville, IN, USA). The standardized composition of Pomella® PFE capsules was fully described [37,38]. The extract was high-performance liquid chromatography (HPLC)-standardized using validated methods and standards to the major pomegranate ellagitannins (30% punicalagin α and punicalagin β) and ellagic acid (5%). Other components, such as gallic acid, caffeic acid, and luteolin, were also identified [37]. The compositional characteristics of PFE capsules (Pomella®) are shown in Table 1.

2.3. Animals

Male Sprague Dawley rats (6-8 week-old, 200 ± 20 g) were purchased from the breeding unit of the Egyptian Organization for Biological Products and Vaccines (Helwan, Egypt). They were housed in an air-conditioned animal unit at 22–25 °C with a 12 h:12 h dark/light schedule and provided with a standard diet and water *ad libitum*. The research protocols of this study complied with the international guidelines for animal use and were approved by the Research Ethics Committee at the Faculty of Pharmacy, Mansoura University, Egypt (ethical approval number: 2022-215).

2.4. Experimental design

Rats were left in cages for one week to adapt. They were then randomly allocated into four groups ($n = 8$/group), as follows: (i) control, received distilled water (3 mL/kg/day, orally); (ii) PFE, received PFE in a daily oral dose of 150 mg/kg suspended in distilled water [41]; (iii) THIO, received THIO (200 mg/kg, i.p, 3 times a week), as previously reported [42] and (iv) [THIO + PFE], received both THIO (200 mg/kg, i.p, 3 times a week) and PFE (150 mg/kg/day, orally). The THIO solution was prepared by dissolving 1 g of THIO in 25 mL of distilled water and rats received 5 mL/kg of this solution. The THIO solution was freshly prepared on the day of injection approximately 1 h before administration. Control groups received the same volume of distilled water. Rats were weighed before each THIO injection to accurately calculate the dose of THIO. THIO was injected in unanaesthetized rats using sterile 25 G syringes. PFE and THIO administration started from day 1 and continued during the whole duration of the experimental protocol (6 weeks).

2.5. Specimen collection and hepatic tissue homogenate preparation

At the end of the experiment, animals were weighed and anesthetized (pentobarbitone sodium, 50 mg/kg, i.p.). Blood samples were collected from the retro-orbital plexus, allowed to clot for 30 min, and centrifuged (1000×*g*/4 °C/10 min (to obtain serum for determination of liver function parameters. Rats were then sacrificed, and a laparotomy was performed to harvest liver, which was rinsed in ice-cold saline, blotted on filter paper, and weighed to calculate liver/body mass index. A portion of the right medial hepatic lobe (100 mg) was maintained in 0.5% KOH for assessment of hydroxyproline content. The left medial lobe was placed in 10% neutral buffered formalin for histopathological and immunohistochemical analyses. A portion of the right lateral hepatic lobe was homogenized (1:10 w/v, 4 °C) in phosphate-buffered saline (pH 7.4) using a tissue homogenizer (Omni TH220, Omni International, USA). The homogenates were centrifuged at 1000×*g* (4 °C/15 min) to obtain supernatants for assessment of oxidative stress and inflammation-related biomarkers, AGE, TGF-β1, TIMP-1, and collagen type IV and laminin or at 10,000×*g* (4 °C/30 min) for determination of hepatic RAGE expression.

2.6. Liver function parameters

Serum levels of alanine aminotransferase (ALT), aspartate aminotransferase (AST), albumin, and total bilirubin were determined using commercial kits from Biodiagnostics (catalog numbers AL1031, AS1061, AB1010 and BR1111, respectively, Badr City, Egypt). Assay kits from Human Diagnostics (Wiesbaden, Germany) were used to assess serum levels of alkaline phosphatase (catalog number 12117, ALP) and lactate dehydrogenase (catalog number 12214, LDH).

2.7. Hepatic oxidative stress

2.7.1. Reduced glutathione (GSH) level and superoxide dismutase (SOD) activity

The hepatic levels of non-protein thiols, mainly GSH, were assessed spectrophotometrically using Ellman's reagent [43]. Additionally, hepatic SOD enzymatic activity was estimated based on its ability to inhibit pyrogallol auto-oxidation at an alkaline pH [44].

2.7.2. Malondialdehyde (MDA) and 4-hydroxynonenal (4-HNE) contents

Hepatic concentrations of MDA and 4-HNE were assessed as previously described [45,46]. Basically, 1-methyl-2-phenylindole reacts with both MDA and 4-HNE in methanesulfonic acid (MSA)-containing medium, forming a stable chromophore (measured at 586 nm; MDA + 4-HNE content). For selective assessment of MDA in presence of 4-HNE, MSA was replaced with hydrochloric acid. Two standard curves were constructed using accurately prepared 1,1,3,3 tetramethoxypropane and 4-HNE (0–20 nmoL/ml) solutions. 4-HNE concentrations were calculated by subtracting MDA values from the total [MDA + 4-HNE] levels.

2.7.3. Reactive oxygen species (ROS)

Hepatic levels of ROS were determined using a fluorometric assay, which is based on ROS-mediated oxidative conversion of stable, non-fluorescent DCFDA to the highly fluorescent dichlorofluorescein (DCF) in the presence of tissue esterases [47]. Excitation was performed at 488 nm and fluorescence was measured at an emission wavelength of 530 nm.

2.8. Hepatic hydroxyproline levels

Hepatic hydroxyproline content was assessed using a colorimetric assay as previously reported [48]. The absorbance of the formed chromophore was read at 550 nm.

2.9. Hepatic AGE fluorescence levels

Hepatic levels of AGEs were determined by quantitative fluorescence spectroscopy, as previously described [49]. Briefly, liver tissue homogenates were diluted (1:30) in 0.1 N NaOH, before centrifugation at 10,000×*g* (4 °C/20 min). Based on their fluorescence

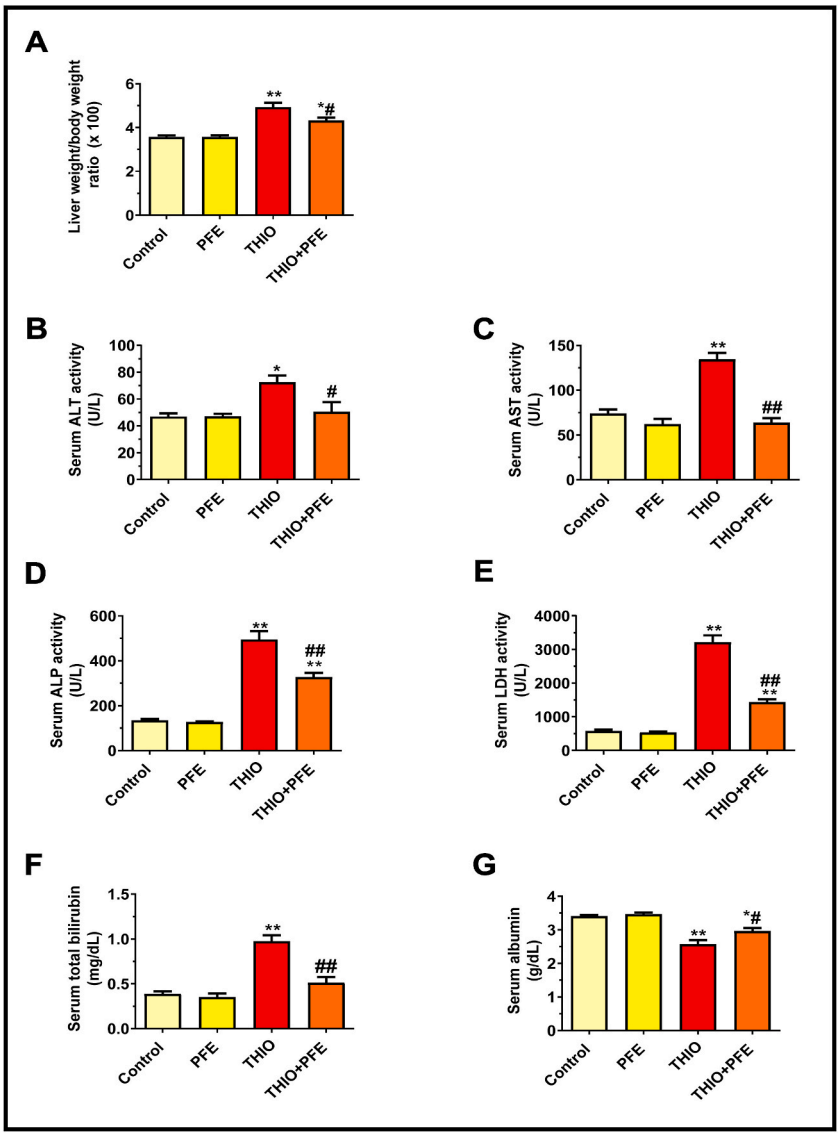

Fig. 1. Effect of pomegranate fruit extract (PFE, 150 mg/kg/day, orally) on liver/body weight index and liver function parameters in thioacetamide (THIO)-administered rats. Data are presented as means ± SEM, $n = 8$/group. *, $P < 0.05$; **, $P < 0.001$ vs. control group. $^{\#}$, $P < 0.05$; $^{\#\#}$, $P < 0.001$ *vs.* THIO group.
ALT, alanine transaminase; AST, aspartate transaminase; ALP, alkaline phosphatase; LDH, lactate dehydrogenase

properties [50–52], AGEs produced a fluorescent signal at a peak emission wavelength of 440 nm when the hepatic supernatant was excited at 370 nm. Fluorescence was determined using a spectrofluorometer (Shimadzu Corporation, Kyoto, Japan). Results were expressed as fluorescence intensity unit (FIU)/mg protein.

2.10. Serum hyaluronic acid (HA) and hepatic levels of AGEs, RAGE, laminin, collagen type IV, TGF-β1 and TIMP-1

Commercially-available Rat ELISA kits were used for the determination of serum HA (catalog number CSB-E08120r, Cusabio, China) and hepatic levels of AGEs (catalog number CSB-E09413r, Cusabio, China), RAGE (catalog number EK0971, PicoKine™, Boster Biological Technology, CA, USA), laminin (catalog number MBS824860, MyBioSource, California, USA), collagen type IV (catalog number SEA180Ra, Cloud-Clone Corp, Houston, TX, USA), TGF-β1 (catalog number 501125468, Platinum, eBioscience, San Diego, CA) and TIMP-1 (catalog number BEK1209, Chongqing Biospes Co., Chongqing, China), following the manufacturer's instructions. The intra-assay and inter-assay coefficients of variations (CV%) were less than 10% for all ELISA kits used.

2.11. Histopathological and immunohistochemical evaluation

Formalin-fixed liver tissues were embedded in paraffin wax, sectioned transversely (5 μm), and stained with Hematoxylin & Eosin (H&E) and Masson's trichrome (MT) stains. The analyses were performed microscopically (Leica Imaging Systems, Cambridge, UK). At least 5 different fields of view were examined per each liver specimen. The degree of hepatic fibrosis was evaluated on a 0–6 scale, as previously described [53]. Moreover, the degree of portal inflammation (0–4), focal necrosis and inflammation (0–4), confluent necrosis (0–6), and periportal/periseptal interface hepatitis (0–4) were semiquantitatively assessed to provide a necroinflammatory activity score for each liver specimen (0–18) [53]. Moreover, the hepatic expression of α-smooth muscle actin (α-SMA) protein was detected immunohistochemically using a mouse monoclonal anti-α-SMA antibody (catalog number MS-113-R7, Thermo Fisher Scientific, UK). Three to five non-overlapping fields were analyzed using ImageJ software (version 1.53t, National Institutes of Health) to quantify the average percentage area of positive immunostaining for α-SMA in each liver specimen, as reported previously [54]. The pathologist performing histopathological assessments was unaware of the group assignment.

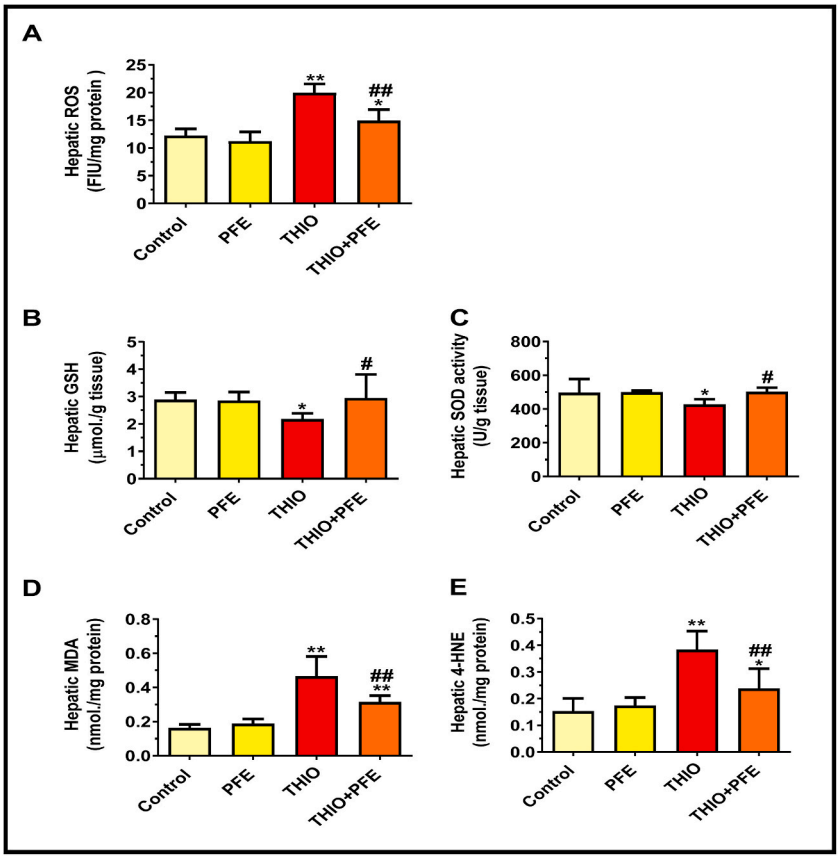

Fig. 2. Effect of pomegranate fruit extract (PFE, 150 mg/kg/day, orally) on hepatic oxidative stress-related parameters in thioacetamide (THIO)-administered rats. Data are presented as means ± SEM, $n = 8$/group. *, $P < 0.05$; **, $P < 0.001$*vs.* control group. #, $P < 0.05$; ##, $P < 0.001$ *vs.* THIO group. ROS; reactive oxygen species; MDA, malondialdehyde; 4-HNE, 4-hydroxynonenal; GSH, reduced glutathione; SOD, superoxide dismutase.

2.12. Statistical analysis

Data are expressed as means ± SEM. To measure significant differences between group means, one-way analysis of variance (ANOVA) followed by Tukey-Kramer's post hoc tests was used. Histopathological fibrosis and necroinflammatory scores were compared using Kruskal-Wallis followed by Dunn's post hoc tests. The significant difference was set at $P < 0.05$. GraphPad Prism Software (V6, San Diego, CA, USA) was used for performing statistical analyses, graphing, and curve fitting of standard curves.

3. Results

3.1. Liver/body weight index and hepatic function parameters

THIO-challenged rats exhibited a significant increase in liver/body weight index (by 1.4 fold, $P < 0.001$) compared to the control group. Daily oral PFE supplementation to THIO-treated rats reduced the liver/body weight ratio by 12.4% relative to the THIO group ($P < 0.05$). These results are shown in Fig. 1A.

Moreover, THIO administration significantly increased serum activities of ALT (by 54.5%, $P < 0.05$), AST (by 81.6%, $P < 0.001$), ALP (by 3.7-fold, $P < 0.001$), and LDH (by 5.6 fold, $P < 0.001$) and serum total bilirubin levels (by 2.5 fold, $P < 0.001$) relative to control rats. Daily administration of PFE to THIO-treated rats significantly diminished THIO-induced elevations in serum ALT (by 30.5%, $P < 0.05$), AST (by 52.5%, $P < 0.001$), ALP (by 33.9%, $P < 0.001$), LDH (by 55.4%, $P < 0.001$) and total bilirubin (by 47.4%, $P < 0.001$) compared to THIO-group (Fig. 1B–F).

THIO-treated rats also exhibited significantly reduced serum albumin levels (by 24.3%, $P < 0.000$; Fig. 1G) in comparison to control animals. PFE supplementation significantly increased serum albumin levels in THIO-treated rats by 16.4% ($P < 0.05$ versus the THIO group).

3.2. Hepatic oxidative stress-related parameters

THIO-administered rats showed a significant increase in hepatic ROS levels (by 1.8-fold, $P < 0.001$ *vs.* control group; Fig. 2A). Moreover, liver tissues from the THIO group showed significant reductions in hepatic GSH and SOD by 24.5% and 14.0%, respectively, compared to the control group (Fig. 2B and C, respectively). This prooxidant/antioxidant imbalance resulted in a marked increase in lipid peroxidation of liver tissues, as indicated by significantly higher hepatic levels of MDA and 4-HNE, biomarkers of lipid peroxidation, by 2.9 and 2.5 fold, respectively, relative to control rats ($P < 0.001$, Fig. 2D and E respectively). Daily oral PFE treatment of THIO-administered rats significantly increased hepatic GSH and SOD by 35.6% and 17.5%, respectively and significantly reduced hepatic levels of ROS, MDA, and 4-HNE by 25.1% 32.6%, and 38.0%, respectively, compared to the untreated THIO rats (Fig. 2A–E).

3.3. Hepatic levels of AGEs and RAGE

Hepatic levels of AGEs (determined by spectrofluorimetric analysis (Fig. 3A) and ELISA (Fig. 3B)) and RAGE (Fig. 3C) were significantly higher in THIO-administered rats relative to the control group ($P < 0.001$). [THIO + PFE]-treated rats showed significantly reduced hepatic AGE concentrations ($P < 0.001$) and RAGE levels (by 42.4%, $P < 0.001$) relative to the untreated THIO group.

3.4. Hepatic expression of TGF-β1 and TIMP-1

Chronic administration of THIO significantly increased hepatic levels of TGF-β1 (by 2.3 fold, $P < 0.001$; Fig. 4A) and TIMP-1 (by 2.3

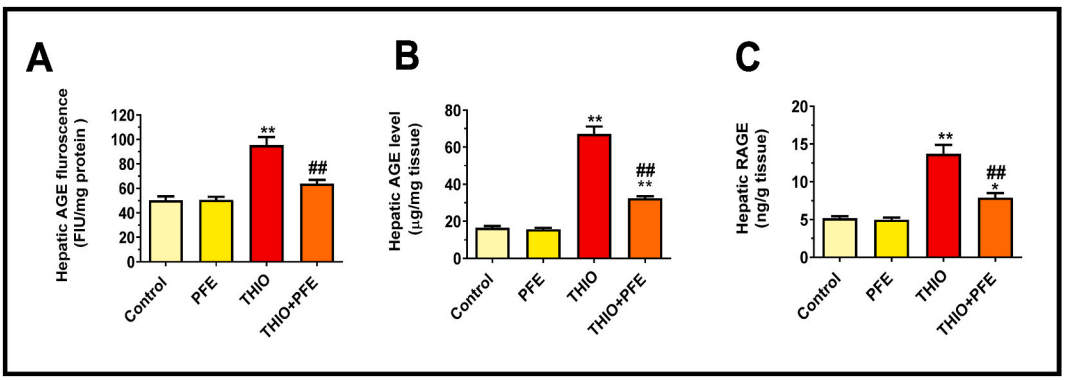

Fig. 3. Effect of pomegranate fruit extract (PFE, 150 mg/kg/day, orally) on hepatic levels of AGEs (A and B) and hepatic RAGE expression (C) in thioacetamide (THIO)-administered rats. Data are presented as means ± SEM, $n = 8$/group. *, $P < 0.05$; **, $P < 0.001$ *vs.* control group. $^{\#\#}$, $P < 0.001$ *vs.* THIO group. AGE, advanced glycation end-products; RAGE, receptors for advanced glycation end-products.

fold, $P < 0.001$; Fig. 4B) relative to the control group. PFE administration to the THIO rats significantly decreased hepatic TGF-β1 (by 23.0%, $P < 0.05$) and TIMP-1 (by 41.5%, $P < 0.001$) levels relative to untreated THIO-group.

3.5. Hepatic α-SMA expression

Hepatic α-SMA expression in control (Fig. 5A) and PFE (Fig. 5B) groups was limited to the vascular walls. However, liver tissues from THIO rats (Fig. 5C) showed marked α-SMA staining in the sinusoidal walls around the central vein and the portal tract. PFE treatment greatly reduced α-SMA hepatic sinusoidal expression in THIO-administered rats (Fig. 5D and E).

Representative photomicrographs (magnification 200 ×) of control (A), PFE (B), THIO (C), and THIO + PFE (D) groups are shown. Scale bar, 50 μm. Arrows show positive α-SMA staining in vascular walls. Arrowheads denote α-SMA expression in sinusoidal walls. E. Positive areas of α-SMA immunostaining. Data are presented as means ± SEM, $n = 8$/group. *, $P < 0.05$; **, $P < 0.001$ *vs.* control group. $^{\#\#}$, $P < 0.001$ *vs.* THIO group.

3.6. Serum HA and hepatic levels of hydroxyproline, collagen IV, and laminin

THIO-administered rats showed a significant elevation in serum HA levels (by 3.7 fold, $P < 0.001$; Fig. 6A). Moreover, hepatic tissues from the THIO group exhibited significant 1.8-, 3.8- and 2.9-fold increases in hydroxyproline ($P < 0.001$, Fig. 6B), collagen type IV ($P < 0.001$, Fig. 6C) and laminin ($P < 0.001$, Fig. 6D), respectively, in comparison to control tissues. PFE treatment significantly attenuated THIO-mediated increases in serum HA (by 41.3%) and hepatic levels of hydroxyproline (by 26%), collagen type IV (by 44.3%), and laminin (by 43.4%).

3.7. Hepatic histopathology

The effects of PFE supplementation on hepatic histopathological changes in THIO-treated rats are shown in Fig. 7. Livers from control and PFE groups showed normal morphology and histological architecture. However, multiple nodules were macroscopically evident on the surfaces of livers from the THIO group. Moreover, Chronic THIO administration elicited marked septal/portal inflammation, interface hepatitis, focal necrosis, collagen deposition, large fibrous septa formation, and incomplete-complete cirrhosis. PFE administration decreased hepatic nodule incidence. Additionally, hepatic tissues from the THIO + PFE group only exhibited mild portal inflammation and reduced extent of fibrosis.

The semiquantitative scores for hepatic necroinflammation (5–8, median = 6) and fibrosis (4–6; median = 6) in THIO rats were significantly higher than those of control rats. For the THIO + PFE group, the necroinflammatory scores (2–4; median = 3) and fibrosis grade (2–6; median = 3.5) were lower than those of the non-treated THIO-administered group, indicating hepatoprotective effects of PFE against THIO-induced damage. These results are shown in Fig. 8.

4. Discussion

In the present study, the potential hepatoprotective influences of PFE against THIO-induced liver fibrosis in rats were investigated. Chronic treatment with PFE ameliorated hepatic dysfunction and markedly halted the development of liver injury and fibrogenesis in THIO-administered rats via exerting antioxidant, anti-inflammatory, and antifibrotic effects. The beneficial influences of PFE in this research were associated with the attenuation of the components of the AGE-RAGE-ROS signaling.

THIO is a powerful liver toxicant that is commonly used to induce liver fibrosis in rodents [55–57]. Chronic THIO administration elicits peri-portal (zone 1) and peri-central (zone 3) fibrosis. Compared to other chemical-based fibrosis models, THIO is associated

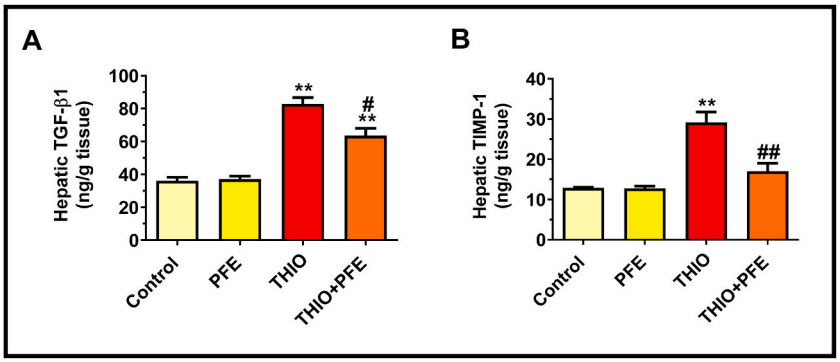

Fig. 4. Effect of pomegranate fruit extract (PFE, 150 mg/kg/day, orally) on hepatic expression of TGF-β1 and TIMP-1 in thioacetamide (THIO)-administered rats.
Data are presented as means ± SEM, $n = 8$/group. **, $P < 0.001$ *vs.* control group. $^{\#}$, $P < 0.05$; $^{\#\#}$, $P < 0.001$ *vs.* THIO group.
TGF-β1, transforming growth factor-β_1; TIMP-1; tissue inhibitor of metalloproteinase-1.

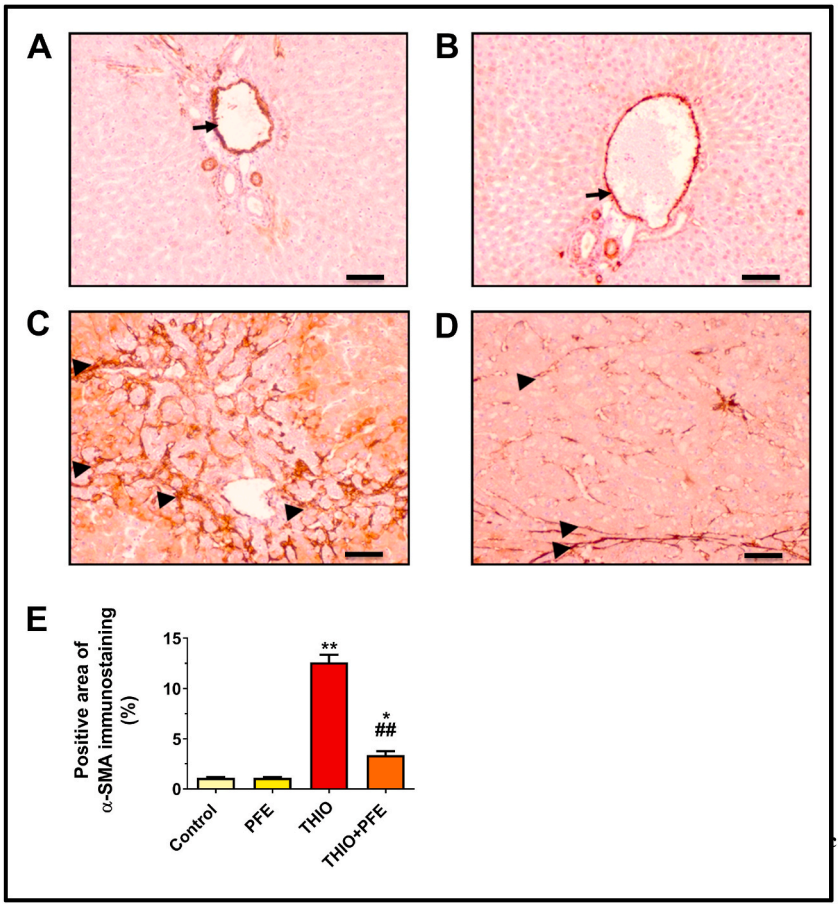

Fig. 5. Effect of pomegranate fruit extract (PFE, 150 mg/kg/day, orally) on hepatic expression of α-smooth muscle actin (α-SMA) in thioacetamide (THIO)-administered rats.

with more pronounced peri-portal injury and inflammatory cell infiltration, quicker development of portal-portal or portal-central bridging septa resembling those occurring in human cirrhosis, and slower spontaneous reversal after THIO withdrawal [58,59]. Moreover, the hepatotoxic effects of THIO are attributed to the covalent binding of its reactive metabolites, THIO sulfoxide and THIO-S, S-dioxide, to cellular macromolecules, an event that eventually triggers hepatic oxidative stress [60,61]. Taken together, these aspects make the THIO model more suitable for the evaluation of the central mechanisms of hepatic fibrogenesis and the screening of potential antifibrotic therapies, particularly those with putative antioxidant properties [58]. Furthermore, THIO-induced liver fibrosis is closely related to alcoholic hepatic disease in terms of histological and metabolic irregularities commonly observed in alcoholic patients [62,63].

In the present study, THIO administration resulted in the typical manifestations of liver function impairment. THIO-induced elevations in serum levels of hepatic enzymes denote liver cell membrane damage [56,64]. THIO-induced oxidative injuries cause a leak of ALT, AST, ALP, and LDH enzymes into the serum, leading to increases in their serum levels [65,66]. Hyperbilirubinemia might be attributed to liver failure to conjugate and excrete bilirubin in the bile, the escape of conjugated bilirubin from the necrotic hepatocytes to sinusoids, and/or hepatobiliary damage [57,64]. Moreover, the reduced serum levels of albumin brought about by THIO administration may be related to an attenuation of hepatocyte synthetic capability [56,67]. Hypoalbuminemia is indicative of the progress of liver damage to a chronic state [64]. PFE supplementation to the THIO group significantly diminished the escape of hepatic enzymes from hepatocytes into the blood and efficiently restored serum albumin concentration to near-normal levels, suggesting that PFE lessened the injurious effects of THIO on rat hepatocytes, halted the deterioration in hepatocyte structure and function and restored the normal hepatocellular synthesis capacity.

THIO-treated rats also showed significantly elevated relative liver weight/body weight index compared to the control group, which may be attributed to increased deposition of ECM proteins in hepatic parenchyma [65,68]. In line with this, THIO-fibrotic rats showed elevated serum levels of HA, a biomarker of fibrosis in chronic liver diseases [69]. Moreover, hepatic tissues from the THIO group showed significant elevations in hydroxyproline, laminin, and collagen IV levels, in comparison to control tissues. Hydroxyproline is an established marker of collagen accumulation [70]. PFE administration to THIO-administered rats resulted in significant reductions in the liver mass index, serum HA, and hepatic ECM protein levels relative to untreated THIO rats, indicating that PFE may attenuate

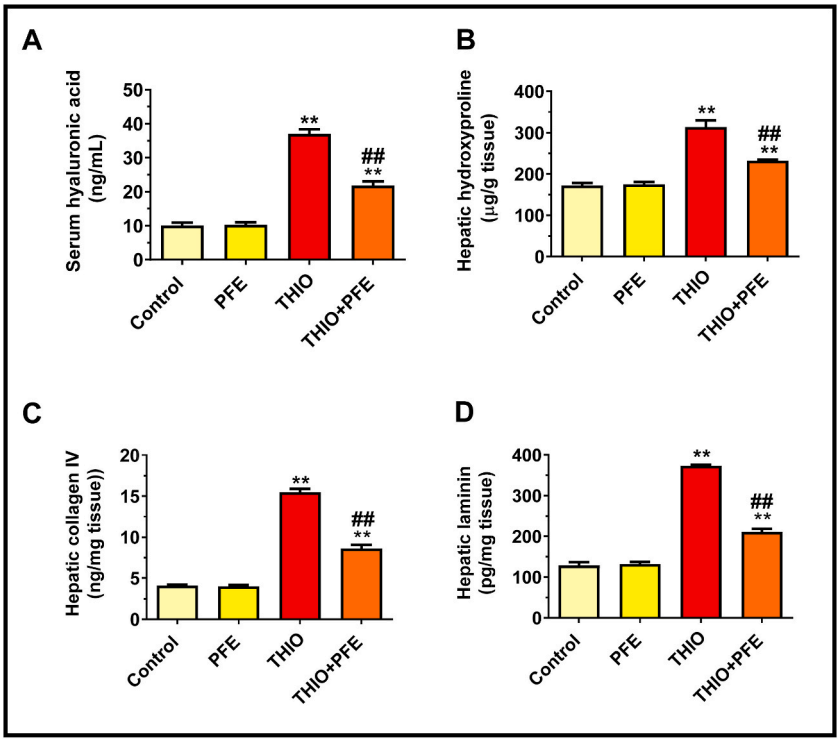

Fig. 6. Effect of pomegranate fruit extract (PFE, 150 mg/kg/day, orally) on serum levels of hyaluronic acid and hepatic levels of hydroxyproline, collagen IV, and laminin in thioacetamide (THIO)-administered rats. Data are presented as means ± SEM, $n = 8$/group. **, $P < 0.001$ *vs.* control group; ##, $P < 0.001$ *vs.* THIO group.

THIO-induced hepatic ECM accumulation.

Data from histopathological analyses of H&E- and MT-stained hepatic tissues also showed that PFE attenuated THIO-induced collagen deposition and disrupted architecture. Moreover, the beneficial effects of PFE in this study involved the inhibition of fibrosis-associated necroinflammation in THIO rats. The necroinflammatory score represents a well-validated histopathological evaluation of the severity of four necroinflammatory features; interface hepatitis, confluent necrosis, focal necrosis, and portal inflammation [53,71]. Chronic hepatic necroinflammation contributes to the development and progression of liver fibrosis via the upregulation of proinflammatory mediators that activate HSCs [72,73]. Supporting this notion, activated HSCs were detected close to areas of lobular necroinflammation in patients with chronic hepatitis C [74]. It is established that chronic necroinflammatory activity inevitably leads to liver fibrosis [75]. Moreover, several reports showed an association between the degree of necroinflammatory activity and the progression of liver fibrosis to cirrhosis [76–78].

Hepatic levels of AGEs and RAGE expression were significantly elevated in THIO rats compared to control levels. Similarly, the hepatic expression levels of RAGE mRNA and protein were significantly increased (by 6–7 fold) in 6-week carbon tetrachloride (CCl4)-treated rats relative to control tissues [21]. Several studies showed that RAGE expression in HSCs is increased during the HSC transition to MF phenotype [11–14]. Increased hepatic expression of α-SMA in liver tissues of THIO rats indicates enhanced levels of HSC activation [79,80]. AGE-RAGE interaction was reported to trigger fibrotic changes in HSCs by increasing ROS generation and enhancing the expression of α-SMA and TGF-β1 [17]. RAGE activation has been shown to trigger ROS generation by activated HSCs via activation of NOX enzymes [14], which also activate NF-κB-mediated inflammation and other signaling pathways [81,82]. Supporting this notion, chronic consumption of a high fat/high fructose/high cholesterol (HFHC) diet enriched with dietary AGEs in mice elicited more severe hepatic oxidative stress and liver fibrosis than in mice only fed on the HFHC diet via a RAGE-dependent pathway [83]. It might be also possible that RAGE activation in THIO rats occurred via engagement with its other ligands such as high-mobility group box 1 protein (HMGB1) and/or members of the S100 family, which have been shown to activate RAGE in animal models of liver fibrosis [20,84,85].

Consistent with increased RAGE expression in fibrotic hepatic tissues, our results showed that chronic THIO-intoxication leads to a substantial imbalance of antioxidant–prooxidant status in the liver milieu. The THIO administration enhanced hepatic ROS generation, which may explain the significant elevation of lipid peroxidation parameters (MDA and 4-HNE) in hepatic tissues. THIO also suppressed hepatic antioxidant mechanisms (GSH and SOD). ROS could contribute to hepatic fibrosis via the activation of HSCs. These findings are in line with previous results [68,86].

PFE administration significantly reduced hepatic RAGE content in THIO-given rats, an effect that potentially contributed to its antioxidant and hepatoprotective effects. Supporting these findings, PFE reduced serum AGE levels in HFHS-fed mice and inhibited *in*

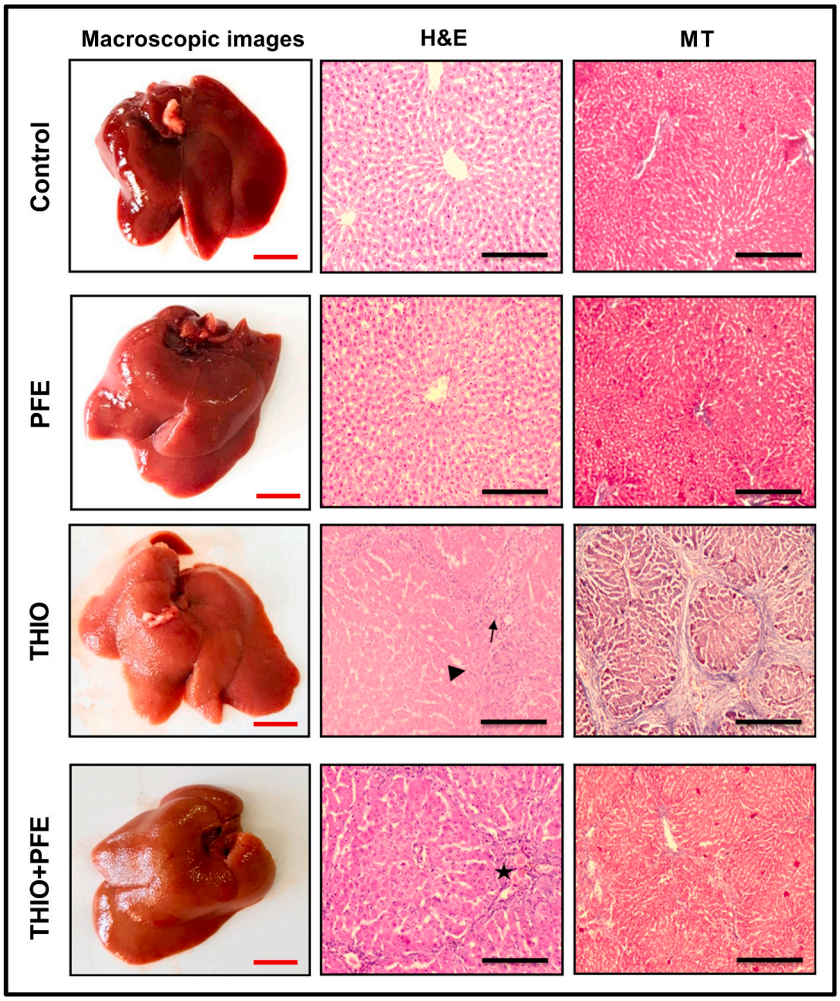

Fig. 7. Effect of pomegranate fruit extract (PFE, 150 mg/kg/day, orally) on hepatic histopathological alterations in thioacetamide (THIO)-administered rats. Representative macroscopic images of whole livers and 100×-magnified photomicrographs of Hematoxylin & Eosin (H&E)- and Masson's trichrome (MT)-stained liver tissues of the study groups are shown. Red scale bars, 1 cm; black scale bars, 100 μm. The arrow denotes septal inflammation, the arrowhead marks interface hepatitis and the star sign shows mild portal inflammation. (For interpretation of the references to color in this figure legend, the reader is referred to the Web version of this article.)

vitro formation of AGEs from bovine serum albumin and sugars [35]. PFE treatment of THIO rats was markedly able to reduce total ROS levels, restore hepatic levels of GSH and SOD antioxidant systems and attenuate hepatic lipid peroxidation. The antioxidant effects of pomegranate-driven products are well-established [33,87,88].

Additionally, hepatic levels of TGF-β1 and TIMP-1 were significantly elevated in THIO-administered rats. Enhanced hepatic levels of TGF-β1 were previously reported in animal models of THIO-induced fibrogenesis [68,89–91]. TGF-β1 was shown to stimulate HSC activation after a set of chronic injuries, increasing the pool of MFs. TGF-β1 was also reported to increase levels of RAGE and α-SMA in MFs [13]. Moreover, it also enhances ECM protein accumulation in pro-fibrogenic cells via several mechanisms including increased expression of TIMP-1 and collagen-I [9,92]. TIMP-1 was previously shown to be overexpressed in activated HSCs and liver tissues exposed to THIO insult [68,93,94]. TIMP-1 inhibits the degradation of ECM components, mitigates apoptosis of MFs, and promotes liver scaring [7,95,96]. THIO-administered animals receiving PFE showed significant reductions in hepatic levels of α-SMA, TGF-β1, and TIMP-1, which may suggest that PFE may halt HSC activation and attenuate hepatic fibrogenesis.

Taken together, the present findings demonstrate that high levels of AGEs, RAGE, and ROS in liver tissues of THIO-fibrotic rats are associated with hepatic lipid peroxidation, necroinflammation, hepatic up-regulation of α-SMA, TGF-β1, and TIMP-1, and hepatic ECM deposition.

Several studies suggested that AGEs-RAGE interaction is a major driver of fibrosis. *In vitro* treatment of cultured HSCs with AGEs increased their proliferation and activation via enhancing ROS generation and intensifying expression of collagen, α-SMA, and TGF-β1 proteins [15,17]. Moreover, the administration of AGEs to bile duct-ligated rats enhanced hepatic oxidative stress, elevated RAGE expression, and augmented liver fibrosis [97]. Exposure of fibroblasts to AGEs resulted in up-regulation of RAGE and TGF-β1

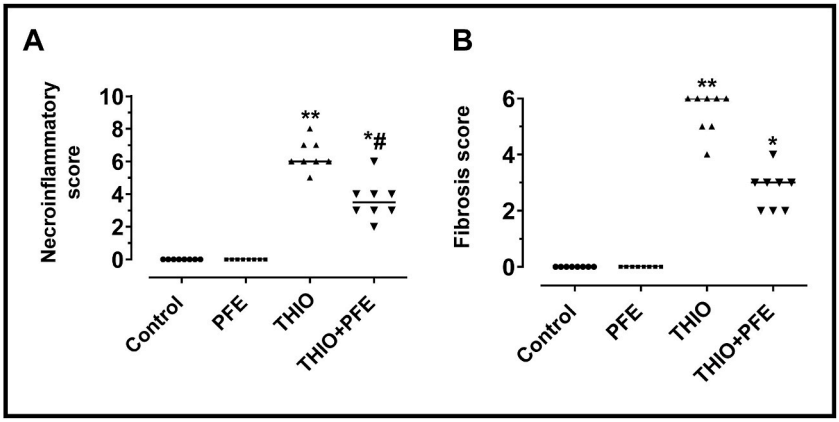

Fig. 8. Grading of histopathological alterations of the hepatic tissues of the study groups. A. A necroinflammatory score for each rat liver was obtained by summing up the activity scores for portal inflammation (0–4), focal necrosis and inflammation (0–4), confluent necrosis (0–6), and interface hepatitis (0–4). B. Fibrosis scores. The median score value for each study group is shown. *, $P < 0.05$; **, $P < 0.001$ *vs.* control group; $^{\#}$, $P < 0.05$ *vs.* THIO group.

expression [98]. Furthermore, inhibition of RAGE signaling via different approaches attenuated experimental liver injury and fibrosis [15–17]. Curcumin diminished AGEs-induced oxidative stress in HSCs by suppressing RAGE expression [99].

Intriguingly, hepatic levels of AGEs, RAGE, and other profibrotic proteins were downregulated by PFE administration. Therefore, we postulated that the molecular mechanism underlying PFE-mediated hepatoprotection against THIO-induced fibrosis is related to the inactivation of the AGE-RAGE-ROS pathway. Yet this speculation needs to be confirmed via other *in vitro* studies that investigate whether PFE can suppress AGEs-induced activation of cultured wild-type HSCs and inhibit their expression of ECM proteins in comparison to PFE effects on HSC cells that lack or overexpress RAGE.

Moreover, our findings suggest that the antifibrotic effects of PFE may begin at early stages of fibrogenesis, namely toxicant-induced liver injury, ROS generation, necroinflammation, profibrotic TGF-β1 overexpression, and HSC activation. Moreover, PFE can also down-regulate ECM protein deposition during the repair process.

A major limitation of the present study is that we investigated the hepatoprotective effects of a single dose of PFE based on the doses reported in the literature. Future research is therefore required to assess the dose-dependent effects of PFE on hepatic fibrogenesis and evaluate the benefits and probable side effects. Another possible limitation might lie in the lack of a standard antifibrotic control in this work. However, up to date, there is no approved antifibrotic drug for the management of hepatic fibrosis disease [5,100]

5. Conclusion

The current study demonstrates that supplementing with PFE in THIO-treated rats has diminished hepatopathological alterations, including necroinflammation and fibrosis development, hepatic dysfunction, oxidative stress, and excessive ECM protein deposition. Our study presents the AGE-RAGE-ROS pathway as a potential target in the molecular mechanisms underlying PFE-mediated effects. The potential use of standardized PFE as a hepatoprotective supplement in patients at high risk of developing liver fibrosis needs to be explored in future clinical studies.

Ethics approval

All applicable international, national, and/or institutional guidelines for the care and use of animals were followed. This article does not contain any studies with human participants performed by any of the authors.

Author contribution statement

Hadeer M. Abouelezz, George S. G. Shehatou: Conceived and designed the experiments; Performed the experiments; Analyzed and interpreted the data; Contributed reagents, materials, analysis tools or data; Wrote the paper.

Abdelhadi M. Shebl: Analyzed and interpreted the data; Contributed reagents, materials, analysis tools or data; Wrote the paper.

Hatem A. Salem: Conceived and designed the experiments; Analyzed and interpreted the data; Contributed reagents, materials, analysis tools or data; Wrote the paper.

Funding statement

This research did not receive any specific grant from funding agencies in the public, commercial, or not-for-profit sectors.

Data availability

The data that support the findings of this study are available on request from the corresponding author. The data are not publicly available due to privacy or ethical restrictions.

Consent to participate

Not applicable.

Declaration of interest's statement

The authors declare that they have no known competing financial interests or personal relationships that could have appeared to influence the work reported in this paper.

List of abbreviations

4-HNE	4-hydroxynonenal
α-SMA	α-smooth muscle actin
AGEs	advanced glycation end products
ALP	alkaline phosphatase
ALT	alanine aminotransferase
ANOVA	one-way analysis of variance
AST	aspartate aminotransferase
DCFDA	2′,7′-dichlorofluorescein diacetate
DCF	dichlorofluorescein
ECM	extracellular matrix
ELISA	enzyme-linked immunosorbent assay
FIU	fluorescence intensity unit
GSH	reduced glutathione
HA	hyaluronic acid
H&E	hematoxylin & eosin
HFHS	high fat/high sucrose
HSCs	hepatic stellate cells
LDH	lactate dehydrogenase
MDA	malondialdehyde
MFs	myofibroblasts
MSA	methanesulfonic acid
MT	Masson's trichrome
NF-κB	nuclear factor-κB
NOX	NAD(P)H oxidase
PFE	pomegranate fruit extract
PPE	pomegranate peel extract
PJ	pomegranate juice
RAGE	receptor for advanced glycation end products
ROS	reactive oxygen species
SOD	superoxide dismutase
TGF-β1	transforming growth factor-β1
THIO	thioacetamide
TIMP-1	tissue inhibitor of metalloproteinase-1

References

[1] C. Liedtke, et al., Liver fibrosis-from mechanisms of injury to modulation of disease, Front. Med. 8 (2021), 814496.
[2] A.E. Toosi, Liver fibrosis: causes and methods of assessment, A review, Rom. J. Intern. Med. 53 (4) (2015) 304–314.
[3] M.-m. Ni, et al., Novel Insights on Notch signaling pathways in liver fibrosis, Eur. J. Pharmacol. 826 (2018) 66–74.
[4] A. Martí-Rodrigo, et al., The antiretroviral rilpivirine induces hepatic regeneration in liver fibrosis and cirrhosis by modulating the STAT3/STAT1 balance, J. Hepatol. 68 (2018) S400.
[5] J.A. Fallowfield, M. Jimenez-Ramos, A. Robertson, Emerging synthetic drugs for the treatment of liver cirrhosis, Expet Opin. Emerg. Drugs 26 (2) (2021) 149–163.
[6] D. Lachowski, et al., Matrix stiffness modulates the activity of MMP-9 and TIMP-1 in hepatic stellate cells to perpetuate fibrosis, Sci. Rep. 9 (1) (2019) 7299.

[7] F.R. Murphy, et al., Inhibition of apoptosis of activated hepatic stellate cells by tissue inhibitor of metalloproteinase-1 is mediated via effects on matrix metalloproteinase inhibition implications for reversibility of liver fibrosis, J. Biol. Chem. 277 (13) (2002) 11069–11076.
[8] H. Wang, et al., Tissue inhibitor of metalloproteinase 1 (TIMP-1) deficiency exacerbates carbon tetrachloride-induced liver injury and fibrosis in mice: involvement of hepatocyte STAT3 in TIMP-1 production, Cell Biosci. 1 (1) (2011) 14.
[9] I. Fabregat, et al., TGF-beta signalling and liver disease, FEBS J. 283 (12) (2016) 2219–2232.
[10] B. Dewidar, et al., TGF-Beta in hepatic stellate cell activation and liver fibrogenesis-updated 2019, Cells 8 (11) (2019).
[11] F. Heinz, et al., Up-regulated expression of the receptor for advanced glycation end products in cultured rat hepatic stellate cells during transdifferentiation to myofibroblasts, Hepatology 34 (5) (2001) 943–952.
[12] C. Lohwasser, et al., Role of the receptor for advanced glycation end products in hepatic fibrosis, World J. Gastroenterol. 15 (46) (2009) 5789–5798.
[13] H. Fehrenbach, et al., Up-regulated expression of the receptor for advanced glycation end products in cultured rat hepatic stellate cells during transdifferentiation to myofibroblasts, Hepatology 34 (5) (2001) 943–952.
[14] E.L. Guimaraes, et al., Advanced glycation end products induce production of reactive oxygen species via the activation of NADPH oxidase in murine hepatic stellate cells, J. Hepatol. 52 (3) (2010) 389–397.
[15] Y. He, et al., Advanced glycation end product (AGE)-induced hepatic stellate cell activation via autophagy contributes to hepatitis C-related fibrosis, Acta Diabetol. 52 (5) (2015) 959–969.
[16] J.W. Park, et al., Increased expression of S100B and RAGE in a mouse model of bile duct ligation-induced liver fibrosis, J. Kor. Med. Sci. 36 (14) (2021) e90.
[17] K. Iwamoto, et al., Advanced glycation end products enhance the proliferation and activation of hepatic stellate cells, J. Gastroenterol. 43 (4) (2008) 298–304.
[18] S. Yamagishi, T. Matsui, Role of receptor for advanced glycation end products (RAGE) in liver disease, Eur. J. Med. Res. 20 (1) (2015) 15.
[19] J. Ji, et al., Liraglutide inhibits receptor for advanced glycation end products (RAGE)/reduced form of nicotinamide-adenine dinucleotide phosphate (NAPDH) signaling to ameliorate non-alcoholic fatty liver disease (NAFLD) in vivo and vitro, Bioengineered 13 (3) (2022) 5091–5102.
[20] P. Xia, et al., Therapeutic effects of recombinant human S100A6 and soluble receptor for advanced glycation end products(sRAGE) on CCl4-induced liver fibrosis in mice, Eur. J. Pharmacol. 833 (2018) 86–93.
[21] J.R. Xia, N.F. Liu, N.X. Zhu, Specific siRNA targeting the receptor for advanced glycation end products inhibits experimental hepatic fibrosis in rats, Int. J. Mol. Sci. 9 (4) (2008) 638–661.
[22] M. Karimi, R. Sadeghi, J. Kokini, Pomegranate as a promising opportunity in medicine and nanotechnology, Trends Food Sci. Technol. 69 (2017) 59–73.
[23] P. Mena, et al., Rapid and comprehensive evaluation of (poly)phenolic compounds in pomegranate (Punica granatum L.) juice by UHPLC-MSn, Molecules 17 (12) (2012) 14821–14840.
[24] Z. Kalaycioglu, F.B. Erim, Total phenolic contents, antioxidant activities, and bioactive ingredients of juices from pomegranate cultivars worldwide, Food Chem. 221 (2017) 496–507.
[25] F. Sharifiyan, et al., Study of pomegranate (Punica granatum L.) peel extract containing anthocyanins on fatty streak formation in the renal arteries in hypercholesterolemic rabbits, Adv. Biomed. Res. 5 (2016) 8.
[26] D. Wang, et al., Vasculoprotective effects of pomegranate (Punica granatum L.), Front. Pharmacol. 9 (2018) 544.
[27] A. Stockton, et al., Effect of pomegranate extract on blood pressure and anthropometry in adults: a double-blind placebo-controlled randomised clinical trial, J. Nutr. Sci. 6 (2017) e39.
[28] M.C. Morzelle, et al., Neuroprotective effects of pomegranate peel extract after chronic infusion with amyloid-beta Peptide in mice, PLoS One 11 (11) (2016) e0166123.
[29] A.E. Ammar, et al., The effect of pomegranate fruit extract on testosterone-induced BPH in rats, Prostate 75 (7) (2015) 679–692.
[30] Y. Deng, et al., The extract from Punica granatum (pomegranate) peel induces apoptosis and impairs metastasis in prostate cancer cells, Biomed. Pharmacother. 93 (2017) 976–984.
[31] Y. Li, et al., Punica granatum (pomegranate) leaves extract induces apoptosis through mitochondrial intrinsic pathway and inhibits migration and invasion in non-small cell lung cancer in vitro, Biomed. Pharmacother. 80 (2016) 227–235.
[32] T. Ganesan, et al., Punicalagin regulates apoptosis-autophagy switch via modulation of annexin A1 in colorectal cancer, Nutrients 12 (8) (2020).
[33] Z. Derakhshan, et al., Antioxidant activity and total phenolic content of ethanolic extract of pomegranate peels, juice and seeds, Food Chem. Toxicol. 114 (2018) 108–111.
[34] A.A.A. Al-Khawalde, et al., Punicalagin Protects against the development of methotrexate-induced hepatotoxicity in mice via activating Nrf2 signaling and decreasing oxidative stress, inflammation, and cell death, Int. J. Mol. Sci. 23 (20) (2022).
[35] Y. Kumagai, et al., Anti-glycation effects of pomegranate (Punica granatum L.) fruit extract and its components in vivo and in vitro, J. Agric. Food Chem. 63 (35) (2015) 7760–7764.
[36] F. de Nigris, et al., The influence of pomegranate fruit extract in comparison to regular pomegranate juice and seed oil on nitric oxide and arterial function in obese Zucker rats, Nitric Oxide 17 (1) (2007) 50–54.
[37] D.-S. Ming, et al., Pomegranate extracts impact the androgen biosynthesis pathways in prostate cancer models in vitro and in vivo, J. Steroid Biochem. Mol. Biol. 143 (2014) 19–28.
[38] S.U. Mertens-Talcott, et al., Absorption, metabolism, and antioxidant effects of pomegranate (Punica granatum l.) polyphenols after ingestion of a standardized extract in healthy human volunteers, J. Agric. Food Chem. 54 (23) (2006) 8956–8961.
[39] S.U. Mertens-Talcott, et al., Absorption, metabolism, and antioxidant effects of pomegranate (Punica granatum L.) polyphenols after ingestion of a standardized extract in healthy human volunteers, J. Agric. Food Chem. 54 (23) (2006) 8956–8961.
[40] C. Patel, et al., Safety assessment of pomegranate fruit extract: acute and subchronic toxicity studies, Food Chem. Toxicol. 46 (8) (2008) 2728–2735.
[41] H. Primarizky, W.M. Yuniarti, B.S. Lukiswanto, Benefits of pomegranate (Punica granatum Linn) fruit extracts to weight changes, total protein, and uric acid in white rats (Rattus norvegicus) as an animal model of acute renal failure, Vet. World 9 (11) (2016) 1269.
[42] M. Nakajima, et al., Nicotine metabolism in liver microsomes from rats with acute hepatitis or cirrhosis, Drug Metab. Dispos. 26 (1) (1998) 36–41.
[43] G.L. Ellman, Tissue sulfhydryl groups, Arch. Biochem. Biophys. 82 (1) (1959) 70–77.
[44] S. Marklund, G. Marklund, Involvement of the superoxide anion radical in the autoxidation of pyrogallol and a convenient assay for superoxide dismutase, FEBS J. 47 (3) (1974) 469–474.
[45] D. Gerard-Monnier, et al., Reactions of 1-methyl-2-phenylindole with malondialdehyde and 4-hydroxyalkenals. Analytical applications to a colorimetric assay of lipid peroxidation, Chem. Res. Toxicol. 11 (10) (1998) 1176–1183.
[46] N.M. Shawky, et al., Comparison of the effects of sulforaphane and pioglitazone on insulin resistance and associated dyslipidemia, hepatosteatosis, and endothelial dysfunction in fructose-fed rats, Environ. Toxicol. Pharmacol. 66 (2019) 43–54.
[47] D. Socci, et al., Evidence that oxidative stress is associated with the pathophysiology of inherited hydrocephalus in the H-Tx rat model, Exp. Neurol. 155 (1) (1999) 109–117.
[48] I. Bergman, R. Loxley, Two improved and simplified methods for the spectrophotometric determination of hydroxyproline, Anal. Chem. 35 (12) (1963) 1961–1965.
[49] C.H. Park, et al., Astaxanthin and Corni Fructus protect against diabetes-induced oxidative stress, inflammation, and advanced glycation end product in livers of streptozotocin-induced diabetic rats, J. Med. Food 18 (3) (2015) 337–344.
[50] G. Münch, et al., Determination of advanced glycation end products in serum by fluorescence spectroscopy and competitive ELISA, Clin. Chem. Lab. Med. 35 (9) (1997) 669–678.
[51] A. Schmitt, et al., Characterization of advanced glycation end products for biochemical studies: side chain modifications and fluorescence characteristics, Anal. Biochem. 338 (2) (2005) 201–215.
[52] A. Piwowar, et al., Plasma glycooxidation protein products in type 2 diabetic patients with nephropathy, Diabetes/Metab. Res. Rev. 24 (7) (2008) 549–553.
[53] K. Ishak, et al., Histological grading and staging of chronic hepatitis, J. Hepatol. 22 (6) (1995) 696–699.

[54] H. Abe, et al., Effective Prevention of liver fibrosis by liver-targeted hydrodynamic gene delivery of matrix metalloproteinase-13 in a rat liver fibrosis model, Mol. Ther. Nucleic Acids 5 (1) (2016) e276.
[55] J. Lee, T. Homma, J. Fujii, Mice in the early stage of liver steatosis caused by a high fat diet are resistant to thioacetamide-induced hepatotoxicity and oxidative stress, Toxicol. Lett. 277 (2017) 92–103.
[56] F.K. El-Baz, A.A.A. Salama, R.A. Hussein, Dunaliella salina microalgae oppose thioacetamide-induced hepatic fibrosis in rats, Toxicol. Rep. 7 (2020) 36–45.
[57] Z.A. El-Gendy, et al., Carvacrol hinders the progression of hepatic fibrosis via targeting autotaxin and thioredoxin in thioacetamide-induced liver fibrosis in rat, Hum. Exp. Toxicol. 40 (12) (2021) 2188–2201.
[58] B. Delire, P. Starkel, I. Leclercq, Animal models for fibrotic liver diseases: what we have, what we need, and what is under development, J. Clin. Transl. Hepatol. 3 (1) (2015) 53–66.
[59] S.C. Yanguas, et al., Experimental models of liver fibrosis, Arch. Toxicol. 90 (5) (2016) 1025–1048.
[60] L. Yuan, N. Kaplowitz, Mechanisms of drug-induced liver injury, Clin. Liver Dis. 17 (4) (2013) 507–5148.
[61] J. Chilakapati, et al., Toxicokinetics and toxicity of thioacetamide sulfoxide: a metabolite of thioacetamide, Toxicology 230 (2–3) (2007) 105–116.
[62] D.K. Ingawale, S.K. Mandlik, S.R. Naik, Models of hepatotoxicity and the underlying cellular, biochemical and immunological mechanism(s): a critical discussion, Environ. Toxicol. Pharmacol. 37 (1) (2014) 118–133.
[63] F. Nozu, N. Takeyama, T. Tanaka, Changes of hepatic fatty acid metabolism produced by chronic thioacetamide administration in rats, Hepatology 15 (6) (1992) 1099–1106.
[64] B. Thapa, A. Walia, Liver function tests and their interpretation, Indian J. Pediatr. 74 (7) (2007) 663–671.
[65] Y.-L. Lin, et al., Hepatoprotective effects of naturally fermented noni juice against thioacetamide-induced liver fibrosis in rats, J. Chin. Med. Assoc. 80 (4) (2017) 212–221.
[66] M.A. Lebda, et al., Melatonin mitigates thioacetamide-induced hepatic fibrosis via antioxidant activity and modulation of proinflammatory cytokines and fibrogenic genes, Life Sci. 192 (2018) 136–143.
[67] G.J. Amirtharaj, et al., Role of oxygen free radicals, nitric oxide and mitochondria in mediating cardiac alterations during liver cirrhosis induced by thioacetamide, Cardiovasc. Toxicol. 17 (2) (2017) 175–184.
[68] N.M. El-Lakkany, et al., Antifibrotic effects of gallic acid on hepatic stellate cells: in vitro and in vivo mechanistic study, J. Tradition. Complement. Med. 9 (1) (2018) 45–53.
[69] O.H. Orasan, et al., Hyaluronic acid as a biomarker of fibrosis in chronic liver diseases of different etiologies, Clujul Med. 89 (1) (2016) 24–31.
[70] R.J. McAnulty, Methods for measuring hydroxyproline and estimating in vivo rates of collagen synthesis and degradation, Methods Mol. Med. 117 (2005) 189–207.
[71] Z.D. Goodman, Grading and staging systems for inflammation and fibrosis in chronic liver diseases, J. Hepatol. 47 (4) (2007) 598–607.
[72] J.P. Iredale, Models of liver fibrosis: exploring the dynamic nature of inflammation and repair in a solid organ, J. Clin. Invest. 117 (3) (2007) 539–548.
[73] S.L. Friedman, Mechanisms of hepatic fibrogenesis, Gastroenterology 134 (6) (2008) 1655–1669.
[74] G.S. Baroni, et al., Hepatic stellate cell activation and liver fibrosis are associated with necroinflammatory injury and Th1-like response in chronic hepatitis C, Liver 19 (3) (1999) 212–219.
[75] R.K. Moreira, Hepatic stellate cells and liver fibrosis, Arch. Pathol. Lab Med. 131 (11) (2007) 1728–1734.
[76] M.G. Ghany, et al., Progression of fibrosis in chronic hepatitis C, Gastroenterology 124 (1) (2003) 97–104.
[77] M. Yano, et al., The long-term pathological evolution of chronic hepatitis C, Hepatology 23 (6) (1996) 1334–1340.
[78] H. Fontaine, et al., Hepatitis activity index is a key factor in determining the natural history of chronic hepatitis C, Hum. Pathol. 32 (9) (2001) 904–909.
[79] K.S. Lee, et al., Pentoxifylline blocks hepatic stellate cell activation independently of phosphodiesterase inhibitory activity, Am. J. Physiol. 273 (5 Pt 1) (1997) G1094–G1100.
[80] H.Q. Jiang, et al., Relationship between focal adhesion kinase and hepatic stellate cell proliferation during rat hepatic fibrogenesis, World J. Gastroenterol. 10 (20) (2004) 3001–3005.
[81] H.S. Park, et al., Cutting edge: direct interaction of TLR4 with NAD(P)H oxidase 4 isozyme is essential for lipopolysaccharide-induced production of reactive oxygen species and activation of NF-kappa B, J. Immunol. 173 (6) (2004) 3589–3593.
[82] S.D. Yan, et al., Enhanced cellular oxidant stress by the interaction of advanced glycation end products with their receptors/binding proteins, J. Biol. Chem. 269 (13) (1994) 9889–9897.
[83] C. Leung, et al., Dietary advanced glycation end-products aggravate non-alcoholic fatty liver disease, World J. Gastroenterol. 22 (35) (2016) 8026–8040.
[84] L.C. Li, J. Gao, J. Li, Emerging role of HMGB1 in fibrotic diseases, J. Cell Mol. Med. 18 (12) (2014) 2331–2339.
[85] X. Ge, et al., High mobility group box-1 drives fibrosis progression signaling via the receptor for advanced glycation end-products in mice, Hepatology 68 6 (2018) 2380–2404.
[86] N.S. Kumar, et al., Oxidative stress in the development of liver cirrhosis: a comparison of two different experimental models, J. Gastroenterol. Hepatol. 21 (6) (2006) 947–957.
[87] M.I. Gil, et al., Antioxidant activity of pomegranate juice and its relationship with phenolic composition and processing, J. Agric. Food Chem. 48 (10) (2000) 4581–4589.
[88] A. Faria, et al., Effect of pomegranate (Punica granatum) juice intake on hepatic oxidative stress, Eur. J. Nutr. 46 (5) (2007) 271–278.
[89] R.S. Palacios, et al., Activation of hepatic stellate cells is associated with cytokine expression in thioacetamide-induced hepatic fibrosis in mice, Lab. Invest. 88 (11) (2008) 1192.
[90] S. Cao, et al., Semen Brassicae ameliorates hepatic fibrosis by regulating transforming growth factor-β1/smad, nuclear factor-κB, and aKT signaling pathways in rats, Drug Des. Dev. Ther. 12 (2018) 1205.
[91] X.-H. Zhang, et al., Blocking follistatin-like 1 attenuates liver fibrosis in mice by regulating transforming growth factor-beta signaling, Int. J. Clin. Exp. Pathol. 11 (3) (2018) 1112–1122.
[92] E. Arendt, et al., Enhanced matrix degradation after withdrawal of TGF-β1 triggers hepatocytes from apoptosis to proliferation and regeneration, Cell Prolif. 38 (5) (2005) 287–299.
[93] J.P. Iredale, et al., Tissue inhibitor of metalloproteinase-1 messenger RNA expression is enhanced relative to interstitial collagenase messenger RNA in experimental liver injury and fibrosis, Hepatology 24 (1) (1996) 176–184.
[94] M.J.P. Arthur, Fibrogenesis II. Metalloproteinases and their inhibitors in liver fibrosis, Am. J. Physiol. Gastrointest. Liver Physiol. 279 (2) (2000) G245–G249.
[95] H. Yoshiji, et al., Tissue inhibitor of metalloproteinases-1 promotes liver fibrosis development in a transgenic mouse model, Hepatology 32 (6) (2000) 1248–1254.
[96] C.J. Parsons, et al., Antifibrotic effects of a tissue inhibitor of metalloproteinase-1 antibody on established liver fibrosis in rats, Hepatology 40 (5) (2004) 1106–1115.
[97] M. Goodwin, et al., Advanced glycation end products augment experimental hepatic fibrosis, J. Gastroenterol. Hepatol. 28 (2) (2013) 369–376.
[98] A.I. Serban, et al., RAGE and TGF-beta1 cross-talk regulate extracellular matrix turnover and cytokine synthesis in AGEs exposed fibroblast cells, PLoS One 11 (3) (2016) e0152376.
[99] J. Lin, et al., Curcumin inhibits gene expression of receptor for advanced glycation end-products (RAGE) in hepatic stellate cells in vitro by elevating PPARgamma activity and attenuating oxidative stress, Br. J. Pharmacol. 166 (8) (2012) 2212–2227.
[100] L. Shan, et al., New drugs for hepatic fibrosis, Front. Pharmacol. 13 (2022), 874408.